European Journal of Pharmaceutics and Biopharmaceutics 135 (2019) 72–82

Contents lists available at ScienceDirect

European Journal of Pharmaceutics and Biopharmaceutics

journal homepage: www.elsevier.com/locate/ejpb

Research paper

Lipodendriplexes: A promising nanocarrier for enhanced gene delivery with minimal cytotoxicity

Imran Tariq[a,b], Shashank Reddy Pinnapireddy[a], Lili Duse[a], Muhammad Yasir Ali[a,c], Sajid Ali[a], Muhammad Umair Amin[a], Nathalie Goergen[a], Jarmila Jedelská[a], Jens Schäfer[a], Udo Bakowsky[a,*]

[a] Department of Pharmaceutics and Biopharmaceutics, University of Marburg, Robert-Koch-Str. 4, 35037 Marburg, Germany
[b] Punjab University College of Pharmacy, University of the Punjab, 54000 Lahore, Pakistan
[c] Faculty of Pharmaceutical Sciences, GC University Faisalabad, Faisalabad, Pakistan

ARTICLE INFO

Keywords:
Liposomes
PAMAM
Dendriplexes
Transfection
Gene therapy
Biocompatible
CAM

ABSTRACT

Non-viral vectors are a safe, efficient and non-toxic alternative to viral vectors for gene therapy against many diseases ranging from genetic disorders to cancers. Polyamidoamine (PAMAM), a positively charged dendrimer has a tendency to complex with nucleic acids (to form dendriplexes) like plasmid DNA (pDNA) and small interfering RNA (siRNA) and can shield them from enzymatic degradation, thereby facilitating endocytosis and endosomal release. In this study, we developed an advanced variant of the dendriplexes by encapsulating them within liposomes to enhance their gene delivery efficiency. This liposome encapsulated dendriplex system can further reduce unwanted cytotoxicity and enhance cellular uptake of nucleic acids. A broad range of lipid combinations were used to optimize the lipodendriplexes in terms of their physicochemical characteristics including size, shape and zeta potential. The optimized lipodendriplexes were tested for pDNA transfection, *in vitro* cell viability, cellular uptake, siRNA mediated knockdown, hemocompatibility, metastatic progression and *in ovo* in chorioallantoic membrane model (CAM). The optimized system has shown significant improvement in pDNA transfection ($p < 0.01$) with higher GFP expression and gene silencing and has shown improved cell viability ($p < 0.05$) compared to the parent dendriplex system. The hemocompatibility and CAM analysis, revealed an efficient yet biocompatible gene delivery system in the form of lipodendriplexes.

1. Introduction

The major objective of *in vivo* gene delivery is to develop a carrier system for the transfer of the gene of interest to the targeted cells with minimal toxic effects [1]. Viruses are by far the most efficient biological vectors to transduce the genetic material into host cells, but the intrinsic immunogenicity and potential toxic effects limit their application in gene therapy [2,3]. On the other hand, free plasmid DNA is unable to cross the cell membrane and is normally degraded in the blood circulation by various intracellular enzymatic pathways [4]. Protective shielding of the negatively charged nucleic acids can be accomplished by electrostatic complexation with positively charged non-viral synthetic vector which can condense the nucleic acid to form stable complexes [5]. These complexes can efficiently cross the cell membrane and release the cargo in the cytosol to achieve the desired therapeutic effect [4].

Among the synthetic non-viral vectors, poly(amidoamine) (PAMAM) dendrimer and polyethylenimine (PEI) are the most extensively used polymers for efficient gene delivery. PAMAM is identified as a safe, non-immunogenic [6], well-characterized cationic system [7,8]. Contrary to PEI, which is a non-degradable polymer (with vinyl bonds in its backbone), PAMAM is a biodegradable polymer (with peptide bonds in its backbone) and is less cytotoxic than PEI [9,10]. It contains several positively charged terminal amino groups that can electrostatically interact with phosphate groups of DNA (to form dendriplexes) and enhance cellular uptake of the complex, via adsorptive pinocytosis [11–13].

However, due to their polycationic nature, they may exhibit some cytotoxicity. On the other hand, they can also interact with oppositely charged macromolecules in plasma like heparin to prematurely displace DNA or RNA from the complex, leading to their enzymatic degradation and lower gene expression [14]. Therefore, non-covalent modification of polymer/DNA complexes with the liposome has been proposed as a useful tool to overcome the demerits associated with the polymeric system.

Liposomal formulations are also well known to deliver a variety of

* Corresponding author.
E-mail address: ubakowsky@aol.com (U. Bakowsky).

https://doi.org/10.1016/j.ejpb.2018.12.013
Received 9 September 2018; Received in revised form 21 December 2018; Accepted 23 December 2018
Available online 24 December 2018
0939-6411/

drugs and genetic materials to the intracellular system [15–17]. Among them, cationic liposomes can deliver the gene of interest more spontaneously. However, the abundance of positive charge may lead to cytotoxicity by inducing some changes at the cellular or even at the chromosomal level, like reduction in mitotic cycle number and increased vacuole formation in the cell cytoplasm [3,18]. While neutrally or negatively charged liposomes are supposed to overcome the cytotoxicity, serum instability, or rapid clearance by the reticular endothelial system, are the major hurdles for the cationic gene delivery vectors. [19]. Negative electrostatic charge repulsion of anionic liposome with the nucleic acid may also lead to poor entrapment of genetic material [20].

The combination of denriplexes and liposomes (lipodendriplexes) can thus improve their individual demerits and help to achieve an enhanced transfection efficiency. Such triblock non-viral vectors exhibit dual interactions viz. with the nucleic acid (dendriplex formation) and also with the negatively charged surface of the cell membrane facilitated by the liposome coated system [21,22]. Thereby, this promising nanocarrier system can enhance intracellular gene delivery with better *in vivo* tolerance [14,23,24].

The aim of the present study was to establish an optimized lipodendriplex system, by using a lipid coated polymer system to exploit the benefits of both, the liposomes (enhanced cellular uptake and low toxicity) and PAMAM dendrimer (optimum nucleic acid complexation, endosomal release) for enhanced gene delivery with minimal toxicity. The formulations were characterised using dynamic light scattering, laser Doppler anemometry and atomic force microscopy. In vitro studies were performed to establish the transfection efficiency using luciferase expression, GFP expression and knockdown assays. MTT assay and hemocompatibility studies were performed to evaluate the biocompatibility of the formulations. *In ovo* studies were carried out using the CAM model.

2. Materials and methods

1,2-dipalmitoylphosphatidylcholine (DPPC), N-[1-(2,3-dioleoyloxy) propyl]-N, N, N-trimethylammonium methylsulfate (DOTAP), 1,2-dipalmitoylphosphatidylglycerol (DPPG), N-(methoxypolyethylene glycol 5000 carbamoyl)-1,2-dipalmitoyl-*sn*-glycero-3-phosphatidylethanolamine (MPEG5000-DPPE) were a kind gift from Lipoid AG (Steinhausen, Switzerland). PAMAM dendrimer, ethylenediamine core, generation 5 solution (5%) in methanol, cholesterol (CH), 4-(2-hydroxyethyl)-1-piperazineethanesulfonic acid (HEPES), 4′,6-diamidino-2-phenylindole (DAPI) and 3-(4,5-dimethylthiazolyl-2)-2,5-diphenyltetrazolium bromide (MTT) were obtained from Sigma Aldrich Chemie GmbH (Taufkirchen, Germany). Dimethyl sulfoxide (DMSO) was purchased from Carl Roth GmbH & Co. Kg (Karlsruhe, Germany). SYBR® Safe DNA dye, Pierce protein BCA assay kit and heparin sodium salt, from porcine intestinal mucosa were purchased from Thermo Fischer Scientific (Dreieich, Germany). Iscove's modified Dulbecco's medium (IMDM), Dulbecco's modified Eagle's minimum essential medium (DMEM), fetal bovine serum (FBS) were purchased from Capricon Scientific (Ebsdorfergrund, Germany). Jet prime transfection reagent was a gift from Polyplus Transfection (Illkirch, France). Purified water from PURELAB flex 2 dispenser (ELGA LabWater, High Wycombe, UK) was used for all the experiments. All other reagents used in experiments were of analytical grade.

2.1. Plasmid DNA and siRNA

Luciferase encoding pCMV-luc and green fluorescence protein encoding pCMV-GFP plasmids were purchased from Plasmid Factory (Bielefeld, Germany). Anti-luciferase siRNA against firefly luciferase gene (sense, 5′-GCC AUU CUA UCC UCU AGA GGA UG-3′) /antisense 3′-CG GUA AGA UAG GAG AUC UCC UAC-5′) and negative control, a non-targeting, non-specific scrambled siRNA (si-Control) to have no silencing effects on rat, mouse and human genes, designed by Dharmacon (Lafayette, USA) were used.

2.2. Cell lines and culturing

A wild-type human ovarian adenocarcinoma (SKOV-3) cell line and human embryonic kidney (HEK-293) cell line were purchased from American Type Culture Collection (ATCC, Manassas, USA). HeLa co-expressing firefly luciferase and GFP under CMV promoter (HeLa LG) was purchased from GenTarget Inc. (San Diego, USA). SKOV-3 cell line was cultured in IMDM (containing 10% FBS at 37 °C and 7% CO_2 under humid conditions). HeLa LG and HEK-293 cell lines were cultured in DMEM (containing 10% FBS at 37 °C and 8.5% CO_2 under humid conditions). All cells were cultivated as monolayers and passaged upon reaching 80% confluency.

2.3. Preparation and optimization of liposomes, dendriplexes, and lipodendriplexes

For the preparation of liposomal formulations, lipids with different molar ratios were dissolved in chloroform/methanol (2:1, v/v). The organic phase was removed by using a rotary evaporator (Heidolph, Germany) and the resulting thin lipid film was rehydrated using 20 mM HEPES buffer (pH 7.4) containing 5% glucose (HBG buffer). The preformed liposomal suspension was sonicated for 10 min in an ultrasonic water bath (Elmasonic P30H, Elma Schmidbauer GmbH, Singen, Germany), to obtain a homogenous suspension. The multilamellar liposomes were slowly extruded (15 ×) through a 100 nm polycarbonate membrane, using a pre-heated Avanti mini extruder (Avanti Polar Lipids, Alabaster, USA) to obtain unilamellar vesicles.

Dendriplexes were formulated at different N/P ratios (the ratio of terminal amino groups in the PAMAM dendrimer to the phosphate groups of the nucleic acid). For the dendriplex formation, pDNA or siRNA solution was added to PAMAM dendrimer solution with vigorous pipetting and incubated for 30 min at room temperature. For the preparation of lipodendriplexes, liposomes at different liposome to PAMAM dendrimer mass ratios (0.1–1) were incubated with dendriplexes for 1 h.

3. Physicochemical characterization

3.1. Dynamic light scattering

The hydrodynamic diameter of the liposomes and of different complexes was measured by dynamic light scattering (DLS) technique using Zetasizer Nano ZS (Malvern Instruments, Malvern, UK). Detection of light scattering was measured at the angle of 173° by an automatically positioned laser attenuator (10 mW HeNe), using a clear disposable folded capillary cell (DTS1060, Malvern Instruments). The samples were diluted (1:100 ratio) using purified water prior to measurement. The average size was calculated with the data of three independent formulations (mean ± standard deviation). The results were expressed as size distribution by intensity.

3.2. Laser doppler anemometry

The zeta potential of the liposomes and of different complexes was measured with laser doppler anemometry (LDA) at a scattering angle of 17° on a Zetasizer Nano ZS. The zeta potential measurements were performed using a clear disposable folded capillary cell (DTS1060). Depending upon the intensity signals of the sample, the instrument automatically performs 15–100 runs per measurement. The average value of the zeta potential was calculated with data of three individual formulations (mean ± standard deviation).

3.3. Gel retardation assay

To check the complex forming ability of pDNA with PAMAM dendrimer, the dendriplexes were subjected to gel electrophoresis using 0.9% agarose gel containing SYBR® safe DNA dye (1:10000 in the 1 × TAE buffer). Dendriplexes containing 0.5 μg of pDNA with varying PAMAM dendrimer ratios (0.5–20) were transferred onto the gel. The gels were subjected to electrophoresis on a Thermo Hybaid Electro 4 (Thermo Electron Corporation, Ulm, Germany) gel system equipped with LKB 2197 constant power supply (LKB Bromma, Bromma, Sweden) set at 80 V for 1 h. The plasmid DNA localization was visualized on a UV transilluminator (Whatmann Biometra, Gottingen, Germany) at a wavelength of 312 nm.

3.4. Fluorescence quenching assay

The intercalation of the pDNA with dendrimer was also evaluated by fluorescence quenching assay. The quenching of the fluorescence of SYBR® safe DNA dye from pDNA, resulting from the complexation with positively charged PAMAM dendrimer, was the signal of the dendriplex formation [25]. Complexes containing 0.5 μg pDNA with SYBR® Safe DNA dye (1:10000 in the buffer) were prepared at different N/P ratios. A microplate reader (FLUOStar Optima, BMG Labtech, Offenburg, Germany) was used for fluorescence measurements at an excitation and emission wavelengths of 502 nm and 520 nm, respectively. The fluorescence measurement of the pDNA complex with SYBR® safe DNA dye without PAMAM dendrimer was considered as 100%. The fluorescence measurement of the complexes was estimated using following equation [20].

$$F_R = (F_{OBS} - -F_D) \times 100/(F_0 - -F_D) \quad (1)$$

F_R depicts relative fluorescence measurement, F_{OBS} is the observed fluorescence of the given sample, F_D is the fluorescence of SYBR® Safe dye without pDNA in HBG buffer, and F_0 is the initial fluorescence without PAMAM dendrimer.

3.5. Atomic force microscopy

Atomic force microscopy was performed on NanoWizard® 3 NanoScience (JPK Instruments, Berlin, Germany). 20 μl of the sample dispersions were placed onto a silicon wafer, fixed on a glass slide, and let to attach with the surface for 10 min. After this, the supernatant was removed and the sample was let to dry. Cantilever tips (NSC14 AlBS, Micromash, Tallinn, Estonia) having a length of 125 mm with a resonance frequency of 160 kHz and nominal force constant of 5 N/m were used. The measurements were carried out in intermittent contact mode (tapping mode) at a scan rate between 0.5 and 1.5 Hz to avoid damaging the samples.

3.6. pDNA transfection and reporter gene knockdown assay

For gene transfection and knockdown assay, cells were seeded at a seeding density of 10 000 cells per well in a 96-well microtiter plates and were allowed to grow overnight before transfection. The complexes containing 0.25 μg pDNA were added in each well, in triplicates, for pDNA transfection studies. For the knockdown assay, complexes containing 7.2 pmol siRNA were used. Additional medium was added after 4 h and plates were evaluated 48 h after transfection.

3.7. Transgene luciferase expression assay

After 48 h incubation period, the complexes were removed and cells were washed twice with phosphate buffer (PBS, pH 7.4) containing calcium (Ca^{2+}) and magnesium (Mg^{2+}). The buffer was then replaced by 50 μl cell culture lysis reagent (CCLR) (Promega, Mannheim, Germany). 20 μl of lysate was then transferred to a 96-well white plate for luciferase reporter gene expression assay. Luciferase assay reagents (Synchem OHG, Felsberg, Germany) were pumped by automatic injection system into each well. Luminiscence was recorded after a 10 s integration time [26].

For protein quantification, Pierce protein BCA assay kit was used, according to the manufacturer's protocol. A portion of 20 μl lysate was transferred to an opaque 96-well microtiter plate and 180 μl of BCA mixture was added to each well. The lysates were incubated at 37 °C for 30 min. The absorbance was measured at 570 nm using a plate reader (FLUOStar Optima) and the values were compared against the bovine serum albumin (BSA) standard curve. The results obtained from these two experiments were expressed as relative luminescence units (RLU) / mg protein.

3.8. In vitro cell viability assay

For *in vitro* cell viability assay, SKOV-3 and HEK-293 cells were seeded at a seeding density of 10 000 cells per well in a 96-well microtitre plate and were incubated overnight. On the following day, the cells were incubated with the complexes; containing 0.25 μg pDNA in each well, for 4 h. 1% Triton™-X100 was used as a positive control. Additional medium was added after 4 h and incubated for further 24 h. The medium was replaced with MTT dye (2 mg/ml) containing medium and incubated for further 4 h. After the incubation, DMSO was added to dissolve the formazan crystals formed by metabolism of the MTT dye by viable cells. The plate was incubated on a shaking incubator (KS4000 IC, IKA Werke, Staufen, Germany) for 15 min. The absorbance of formazan was measured at 570 nm (FLUOStar Optima). The cell viability of the cells was expressed as a percentage of viability in comparison to untreated cells [27,28].

3.9. Ex vivo hemolysis assay

To determine the hemolytic effect of the complex in blood, human erythrocytes were isolated from fresh blood [29]. The blood was transferred into tubes containing EDTA to avoid coagulation and centrifuged to separate the plasma fraction. The erythrocyte pellet was washed thrice with PBS and diluted to 1:50 with PBS. 180 μl of erythrocytes dispersion were mixed with 20 μl complexes, containing 0.25 μg pDNA in a V-bottomed 96-well plate and incubated for 1 h at 37 °C in a shaking incubator. The plates were then centrifuged and the supernatant was collected to measure the absorbance at 540 nm (FLUOStar Optima). PBS, NaCl 0.9% solution, untreated erythrocytes and 1% Triton™ X-100 were used as controls. The absorbance value of 1% Triton™ X-100 was considered as 100% hemolysis [30,31].

3.10. Natural polyanion heparin competition assay

The pDNA stability of the dendriplexes and lipodendriplexes, against the natural polyanion (heparin) was evaluated by heparin competition assay. The complexes containing 0.25 μg pDNA, were used for analysis and incubated for 30 min with decreasing amounts of heparin. The complexes were then loaded onto 0.9% agarose gel containing SYBR® safe DNA dye and subjected to electrophoresis for 1 h at 80 V and visualized using a UV *trans*-illuminator at 312 nm [32,26].

3.11. Cellular uptake studies

For the visualization of cells and GFP reporter gene expression analysis, SKOV-3 and HEK-293 cells were seeded in 12 well- cell culture plates (Nunclon Delta, Nunc GmbH & Co. KG., Wiesbaden, Germany) containing coverslips (15 mm diameter) at the seeding density of 90 000 cells per well. After 24 h, the complexes containing 2 μg of pCMV-GFP were added dropwise into each well and incubated for 4 h. After incubation, additional medium was added to the wells and incubated up to 48 h. The cells were washed thrice with 300 μl ice-cold PBS

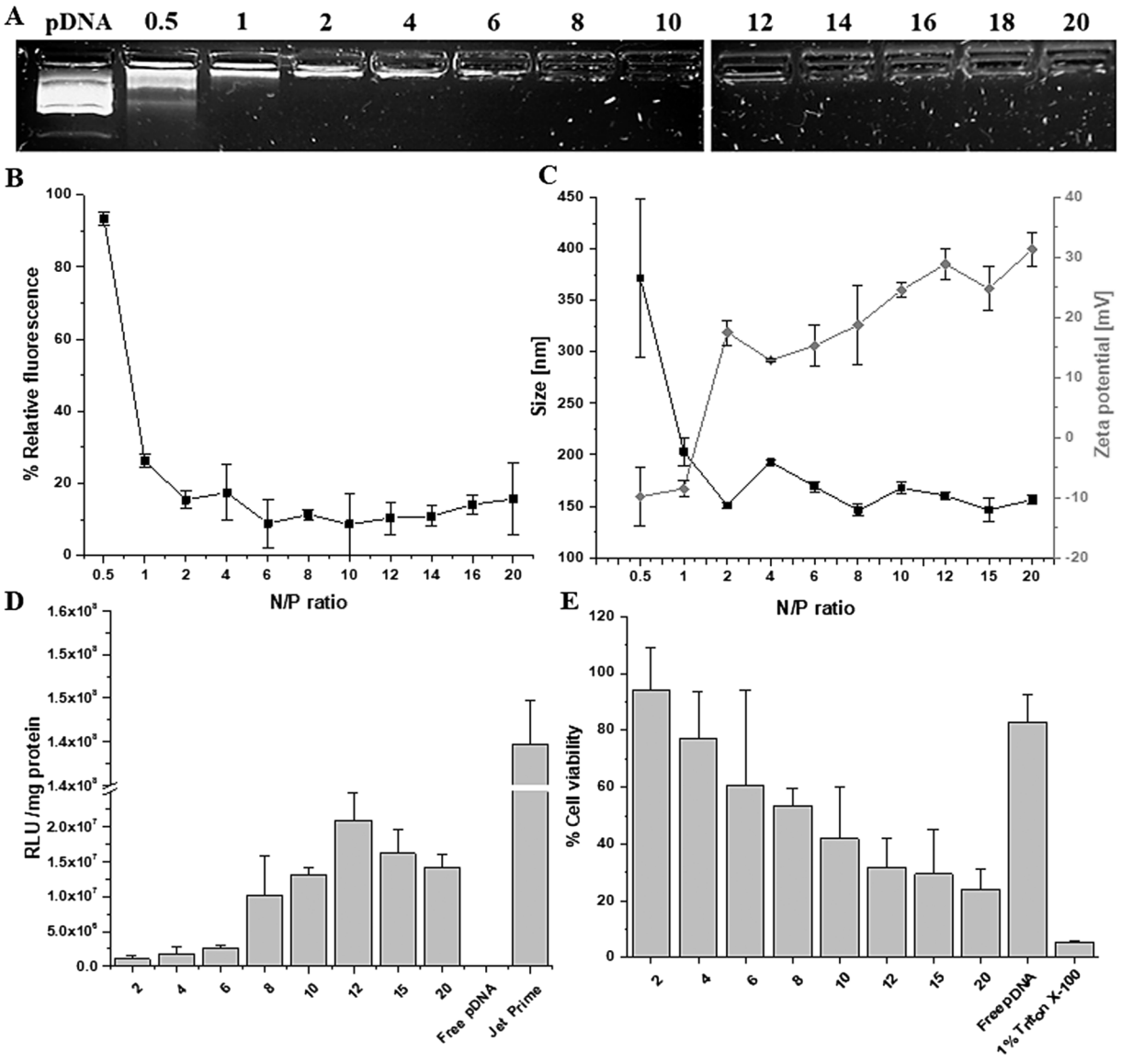

Fig. 1. (A) Gel retardation assay: gel electrophoresis of dendriplexes at varying N/P ratios from 0.5 to 20, showing complex formation at N/P ratio 2 with no band on the gel. Free pDNA was used as a control. (B) Fluorescence quenching assay: relative fluorescence at different N/P ratios showed a decrease in fluorescence with increase in N/P ratio. About 85% fluorescence was reduced at N/P ratio 2 indicating the start of complex formation. (C) Size and zeta-potential of dendriplexes at different N/P ratios prepared in HBG buffer (pH 7.4) after 30 min of incubation. (D) pDNA transfection and (E) cytotoxicity studies of dendriplexes at different N/P ratios in HEK-293 cell line, Jet Prime and 1% Triton™-X 100 as positive controls for the respective experiments. Values are represented as means ± S.D.

containing Ca^{2+} and Mg^{2+}. The cells were then fixed with 300 µl of 4% formaldehyde solution, followed by incubation for further 20 min at room temperature. The cell nucleus was counterstained with DAPI (0.1 µg/ml). The cells were then washed with PBS containing Ca^{2+} and Mg^{2+} and the coverslips were placed onto a clear glass slide and sealed with fluorescence-free glycerol-based mounting medium (FluorSave™, Calbiochem, San Diego, USA). Finally, the cells were analysed under a microscope (CKX-53 Olympus, USA), equipped with fluorescence detection filters for GFP (ex.505 nm–em.530 nm) and DAPI (ex.385–em.470 nm).

3.12. Chorioallantoic membrane (CAM) assay

Fertilized eggs were purchased from Mastkükenbrüterei Brormann (Rheda-Wiedenbruck, Germany). The eggs were disinfected with 70% ethanol and incubated in an egg hatching incubator, equipped with an automatic rotator (rotation after every 4 h) at a temperature of 37 °C with a relative humidity of about 60%. On the egg development day (EDD) 4, a hole of 30 mm diameter was made into eggshell using a pneumatic egg punch (Schuett Biotech, Germany), to expose the CAM surface. The exposed part of the egg was then covered with a small Petri dish and placed back into the incubator. On the EDD 11, 50 µl of dendriplexes or lipodendriplexes containing 0.5 µg of pCMV-GFP were injected, under the stereomicroscope (Stemi 2000-C, Carl Zeiss GmbH, Germany), into the mesoderm of CAM, with the help of glass cannulas. The eggs were further incubated for 48 h. On EDD 13, about 1 cm of the CAM was dissected and placed on clear glass slide after washing with 0.9% NaCl. Finally, the GFP expression was observed under a confocal laser scanning microscope (Zeiss LSM 700, Carl Zeiss GmbH, Jena, Germany).

3.13. Metastatic progression assay

SKOV-3 cells were grown in 24-well cell culture plates at a seeding density of 50 000 cells per well. The complexes containing 1 µg of pCMV-luc were added to each well. Cells were transfected for 4 h in

Table 1
Size and zeta potential (mean ± SD) of different liposomal formulations.

Formulations (mol:mol)	Size ± S.D [nm] (PDI)	Zeta potential ± S.D [mV]
DPPC:CH (85:15)	105.2 ± 17.3 (0.12)	−7.5 ± 0.7
DPPC:CH:MPEG5000-DPPE (85:14:1)	128.7 ± 59.8 (0.23)	−17.9 ± 11.2
DPPC:DPPG (92:8)	107.1 ± 32.8 (0.15)	−14.0 ± 2.5
DPPC:DOTAP (95:5)	87.8 ± 12.7 (0.15)	+35.8 ± 5.8
DPPC:DOPE:CH (45:40:15)	109.2 ± 22.2 (0.19)	−12.6 ± 2.0
DPPC:MPEG5000-DPPE (95:5)	125.6 ± 68.5 (0.21)	−22.5 ± 2.2

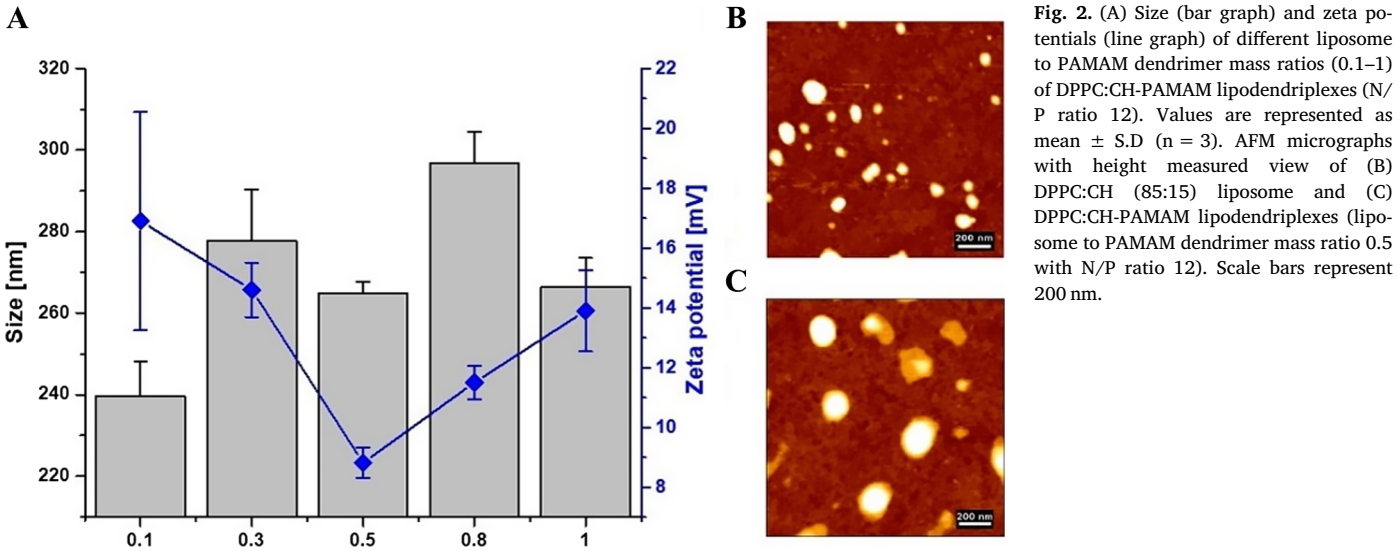

Fig. 2. (A) Size (bar graph) and zeta potentials (line graph) of different liposome to PAMAM dendrimer mass ratios (0.1–1) of DPPC:CH-PAMAM lipodendriplexes (N/P ratio 12). Values are represented as mean ± S.D (n = 3). AFM micrographs with height measured view of (B) DPPC:CH (85:15) liposome and (C) DPPC:CH-PAMAM lipodendriplexes (liposome to PAMAM dendrimer mass ratio 0.5 with N/P ratio 12). Scale bars represent 200 nm.

serum-free medium. Wound healing assay was performed by making a scratch in the middle of each well with a 100 µl sterile pipette tip. Samples were washed twice with PBS to remove the cell debris and incubated with the medium containing 10% FBS. Cells of each sample were photographed at indicated time intervals (0, 16, 24 and 48 h) from three different positions (CKX-53 Olympus, USA). The images were analyzed using Wimasis image analysis software (Onimagin Technologies SCA, Córdoba, Spain). The migration rate was expressed as a percentage of the scratch closure area.

3.14. Statistical analysis

All experiments were performed in triplicates and the values are mentioned as a mean ± standard deviation. One way Anova was performed to identify statistically significant differences using IBM SPSS software (Ver. 22). Dunnett's test was used for multi- comparison between the results and control, whereas multi-comparison among the different groups was made using Tukey's test. Probability values of $p < 0.05$ were considered significant. Statistical significances are indicated as $^{*}p < 0.05$, $^{**}p < 0.01$, $^{***}p < 0.001$.

4. Results and discussion

4.1. Physicochemical characterization and optimization of dendriplexes

The characterization of dendriplexes is the prerequisite of lipodendriplex formation. It has been reported that PAMAM dendrimer of generation 5, has all of its 128 primary amines in protonated form at physiological pH, and thus can electrostatically interact with the negatively charged nucleic acid to form dendriplexes [33]. To check the stable complex formation of PAMAM dendrimer with pDNA, N/P ratios from 0.5 to 20 were selected and analysed using gel electrophoresis and fluorescence quenching assay. Gel electrophoresis reveals that at N/P ratio 2, stable complex formation occurs, showing no DNA band on the gel (Fig. 1A). Similar findings were observed by Movassaghian et al. [23].

Further analysis with fluorescence quenching assay, indicated similar results. The quenching in relative fluorescence was observed upon the increase in N/P ratio (Fig. 1B). The results suggested the maximum complexation at N/P ratio 2 which is indicated by the reduction in fluorescence intensity. This also suggests that the PAMAM dendrimer's binding on pDNA was very strong and that the dendrimer cannot be displaced by addition of the dye. A saturation point was then attained indicating a state of equilibrium [34].

The size and zeta potential of the dendriplexes were measured by DLS and LDA, respectively. It was observed that with an increase in N/P ratio from 0.5 to 2, the size of the complexes decreased and the zeta potential changed from negative to positive, due to the decrease in pDNA mobility (as mentioned above). At greater N/P ratios, a state of equilibrium was observed (Fig. 1C). Results showed that dendriplexes have a tendency to form aggregates at a zeta potential close to zero, but stabilized at the higher positive zeta potential. Therefore, sufficiently high zeta potential was crucial for the stability of dendriplexes.

For the optimization of dendriplexes, pDNA transfection and cytotoxicity experiments were performed on HEK-293 cell line [35] using different N/P ratios (Fig. 1D and 1E). It was observed that by increasing the charge ratio, the transfection efficiency was increased, due to an increase in charge interaction between the complexes and the negatively charged surface of the cell membrane. Maximum transfection was observed at N/P ratio 12 as compared to lower N/P ratios. With a further increase in N/P ratio, transfection efficiency dropped. The induction of very high positive charge on the complexes was responsible for enhanced cell membrane disruptions and lower transfection efficiency [36]. The cytotoxicity assay also showed a 50% drop in the viability of the cells at N/P ratio 8 with further increase in toxicity with increasing N/P ratios. Dendriplexes with N/P ratio 12, having a size of

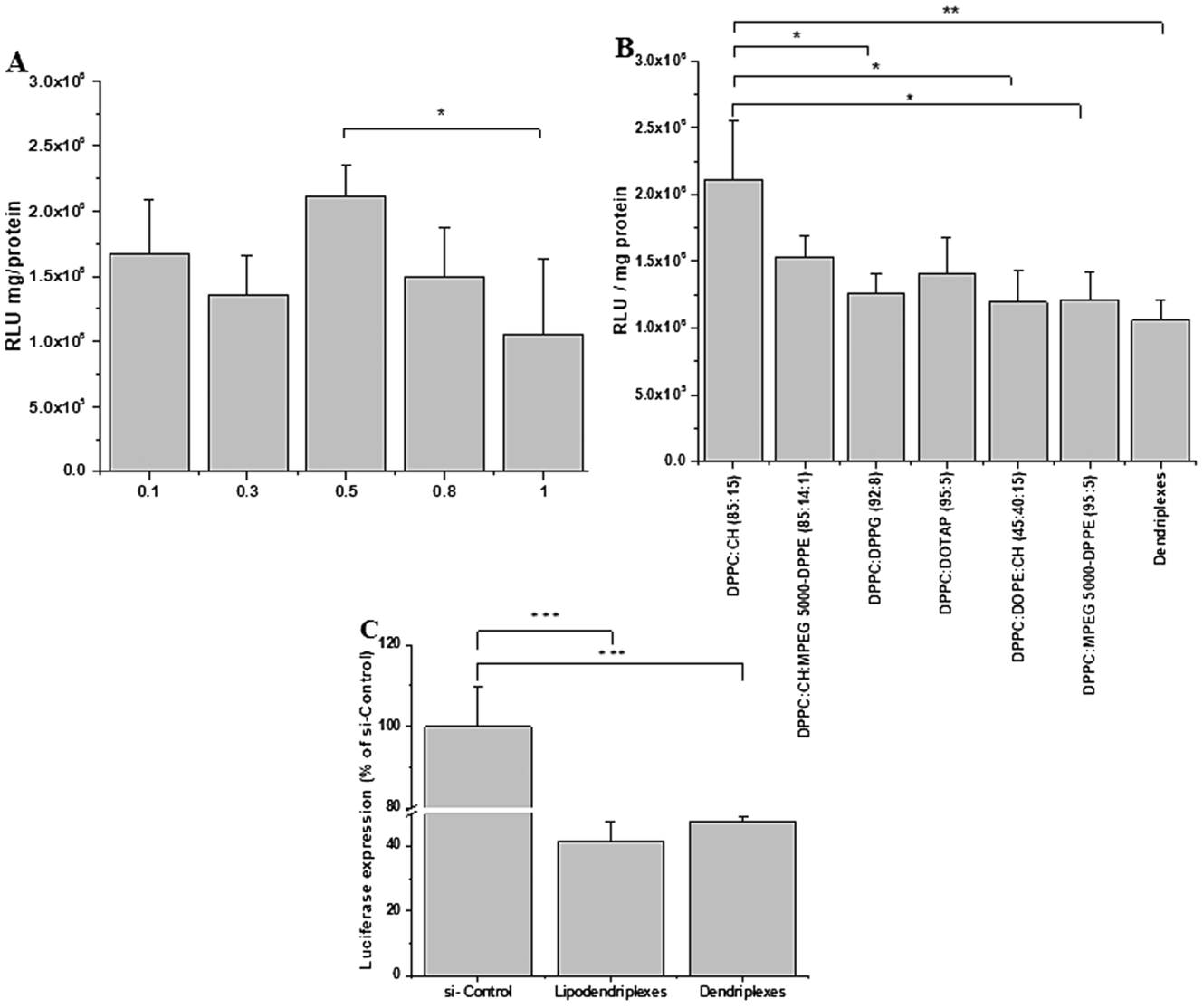

Fig. 3. (A) DNA transfection studies in SKOV-3 cell line with different mass ratios (0.1–1) of DPPC:CH-PAMAM lipodendriplexes (N/P ratio 12) and (B) of lipodendriplexes of different liposome formulations (liposome to PAMAM dendrimer mass ratio 0.5) using N/P ratio 12. (C) The knockdown efficiency in HeLa LG cell line of optimized dendriplexes (N/P ratio 12) and DPPC:CH-PAMAM lipodendriplexes (liposome to PAMAM dendrimer mass ratio 0.5) using N/P ratio 12. Luciferase gene knockdown of the complexes is expressed as the percentage of non-specific control siRNA (si-Control). Values are represented as mean ± S.D (n = 3) and statistical significances are indicated as $^{*}p < 0.05$, $^{**}p < 0.01$, $^{***}p < 0.001$.

160.7 ± 3.5 nm with a zeta potential of 28.9 ± 2.5 mV (suitable for incorporation into liposomes) and the highest transfection efficiency with least toxicity among the three best transfecting N/P ratios were selected for further studies to optimize lipodendriplexes of different liposomal formulations.

4.2. Physicochemical characterization of lipodendriplexes

To find an optimal lipid composition for lipodendriplex formation, different lipids with various molar ratios were investigated. The physicochemical properties of a broad range of liposomal formulations were determined. All the extruded liposomes were of a size range between 87.8 nm and 128.7 nm, with narrow and monodisperse size distribution having a polydispersity index (PDI) of approximately 0.1, except for pegylated liposomes, having a PDI of about 0.2 (Table 1). The zeta potential of the liposomal formulations was in the negative range except the positively charged DPPC:DOTAP (95:5) liposomes.

In order to optimize the stoichiometry of lipodendriplexes, the DPPC:CH (85:15) formulation was initially selected, to complex with optimized dendriplexes. Different liposome to PAMAM dendrimer mass ratios from 0.1 to 1 were tested for lipodendriplex formation. As shown in Fig. 2, the apparent size of the resulting lipodendriplexes increased compared to parent dendriplexes. It was also observed that by increasing the liposome mass ratio from 0.1 to 0.5, zeta potential of the lipodendriplexes decreased showing the maximum liposome shielding over the dendriplexes at a mass ratio of 0.5. The maximum shielding is very important to minimize the PAMAM associated cytotoxicity and unwanted interaction of these complexes with the blood components [37]. With further increase in liposome mass ratio, a slight increase in zeta potential of the complexes was observed, which was due to possible charge competition between negatively charged liposomes and pDNA for the binding sites on the positively charged PAMAM. These changes can cause a slight destabilisation of dendriplexes and expose some of the amino groups to the outer site. The additional positive charge may also lead to lower transfection efficiency with an increase in cytotoxicity, as depicted in Figs. 3B and 4B.

The above mentioned results were in good correlation with the AFM findings. AFM images showed that the pure liposomes were spherical and their size was similar to the hydrodynamic diameter obtained from DLS (Fig. 2B). In case of the lipodendriplexes, the shape of complexes

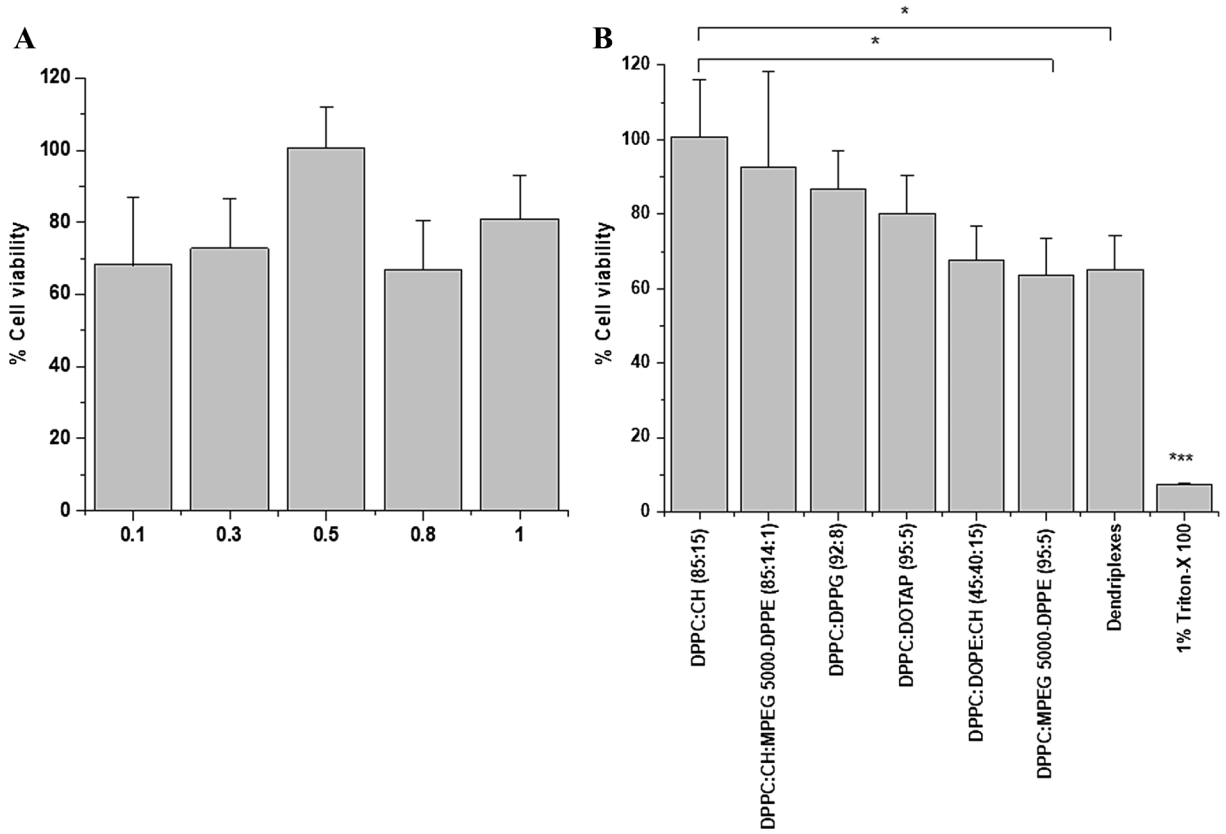

Fig. 4. Cell viability studies in SKOV-3 cell line with (A) different mass ratios (0.1–1) of DPPC:CH-PAMAM lipodendriplexes (N/P ratio 12) and (B) lipodendriplexes of different liposomal formulations (liposome to PAMAM dendrimer mass ratio 0.5) using 1% Triton™-X 100 as a positive control. Values are represented as mean ± S.D (n = 3) and statistical significances are indicated as $^{*}p < 0.05$, $^{***}p < 0.001$.

slightly changed from spherical to slightly oval [38]. This was due to the non-covalent interaction of liposome with dendriplexes. The lipid layer spreading onto the silica surface showed a step height of about 4 nm, representing a lipid bilayer. From Fig. 2C some disrupted lipodendriplexes are evident which might have occurred during the AFM sample preparation, depicting an escape of dendriplexes from their lipid layers.

4.3. pDNA transfection and reporter gene knockdown assay

After the establishment of optimized dendriplexes, the transfection efficiency of lipodendriplexes of DPPC:CH (85:15) using different liposome to PAMAM dendrimer mass ratios (0.1 to 1) was tested in SKOV-3 cell line. It was observed that the liposome to PAMAM dendrimer mass ratio 0.5 showed best transfection results (Fig. 3A). Thereby, this ratio was further tested with lipodendriplexes of different liposomal formulations, in order to optimize the best transfecting formulation (Fig. 3B). Lipodendriplexes of DPPC:CH (85:15), DPPC:CH:MPEG 5000-DPPE (85:14:1) and also of positively charged DPPC:DOTAP (95:5) showed good transfection efficiencies. In contrast, lipodendriplexes of DPPC:CH (85:15) showed a significant improvement in transfection efficiency as compared to lipodendriplexes of DPPC:DPPG (92:8), DPPC:DOPE:CH (45:40:15) and DPPC:MPEG 5000-DPPE (95:5) and of its parent dendriplexes. Surprisingly, DOPE containing lipodendriplexes exhibited lower transfection efficiency, which might be due to a change in the physicochemical properties of the resulting complex, while the large PEG chain containing liposome (DPPC: MPEG 5000-DPPE; 95:5) remarkably reduced the transfection efficiency [37].

Knockdown experiments were performed to determine the gene silencing effect of the formulations. Based on the best transfection efficiency profile, lipodendriplexes of DPPC:CH (85:15) were selected for further experiments of luciferase gene knockdown. The results of gene silencing experiments were similar to those obtained in transfection experiments. Lipodendriplexes showed a slight improvement (insignificant) in the knockdown of the luciferase expressing gene than dendriplexes, as shown in Fig. 3C.

4.4. In vitro cytotoxicity assay

In the case of lipodendriplexes, the liposomal layer, which shields the dendriplex, might inhibit the binding of terminal amino groups to the surface of the cell membrane and thereby create a more favourable environment for the cells and consequently improve cell viability [23]. The lipodendriplexes of DPPC:CH (85:15) with different liposome to PAMAM dendrimer mass ratios (0.1–1), using optimized dendriplexes, were initially tested. It was observed that lipodendriplexes with a liposome to PAMAM dendrimer mass ratio of 0.5 showed the highest cell viability (Fig. 4A). Therefore, this liposome to PAMAM dendrimer mass ratio was further tested with lipodendriplexes of different liposomal formulations. The lipodendriplexes of DPPC:CH (85:15) showed a significant ($p < 0.05$) improvement in cell viability as compared to its respective optimized dendriplexes. The results also depicted a good cell viability profile for lipodendriplexes of DPPC:CH:MPEG 5000-DPPE (85:14:1), DPPC:DOTAP (95:5) and DPPC:DPPG (92:8). While lipodendriplexes of DPPC:DOPE:CH (45:40:15) and DPPC:MPEG 5000-DPPE (95:5) exhibited a lower cell viability profile (Fig. 4B). Therefore, DPPC:CH (85:15) lipodendriplexes were considered to be the best formulation in terms of cell viability. Similar results were described by Schäfer et al. [39].

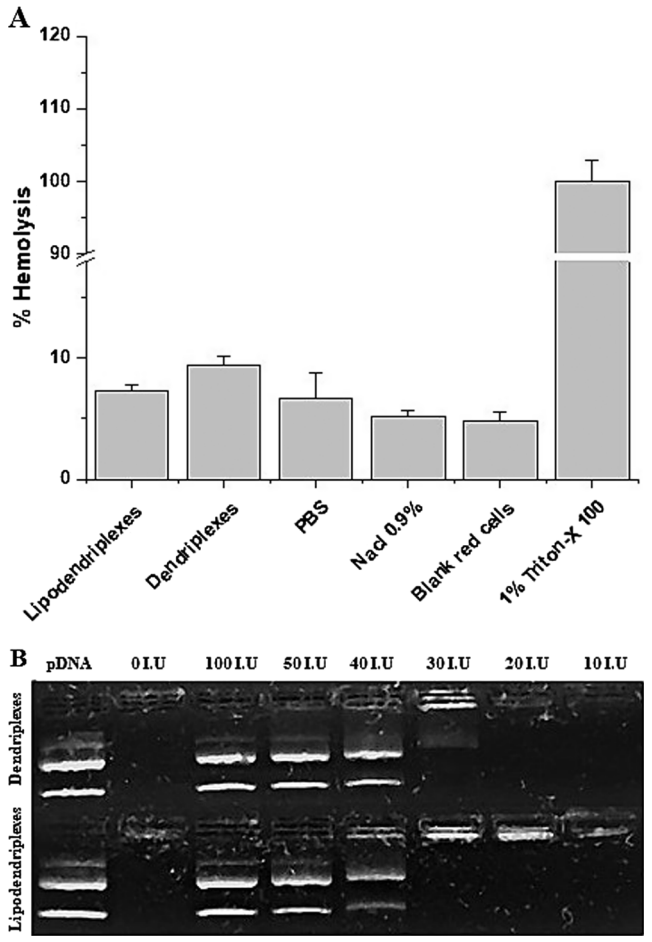

Fig. 5. (A) *Ex vivo* hemolysis assay of optimized dendriplexes (N/P ratio 12) and of DPPC:CH-PAMAM lipodendriplexes (liposome to PAMAM dendrimer mass ratio 0.5, using 1% Triton™-X 100 as a positive control and PBS, NaCl 0.9% solution, untreated erythrocytes as negative controls. Values are represented as mean ± S.D (n = 3). (B) DNA stability studies of optimized dendriplexes (N/P ratio 12) and of DPPC:CH-PAMAM lipodendriplexes (liposome to PAMAM dendrimer mass ratio 0.5) using different heparin concentrations (I.U/100 ml). 0 I.U represents complexes without heparin.

4.5. Ex vivo hemolysis and natural polyanion heparin competition assay

The free terminal amino groups having positive charge contributed to the concentration-dependent hemolytic effect on red blood cells [40], therefore, by increasing the charge ratio, a constant increase in toxicity was recorded. Therefore, the most efficient and less toxic non-viral vectors from pDNA transfection and *in vitro* cytotoxicity experiments were chosen for the hemolysis assay. Optimized lipodendriplexes were very stable and showed hemolysis of about 7.3%, which was less than the hemolysis induced by dendriplexes alone (Fig. 5A).

pDNA stability of the charged complexes is the key factor to evaluate the integrity of the non-viral gene carrier system. The stability of the complexes can be affected by the increasing concentrations of natural polyanions (heparin) that can competitively interact with the oppositely charged PAMAM dendrimer and may result in the initial release of pDNA. Therefore, the stability of the complexes was tested by *in vitro* pDNA stability assay, using heparin as a model molecule. The concentration of heparin in a healthy adult is the range of 5–15 I.U/100 ml [41]. It was observed that the optimized lipodendriplexes exhibited pDNA release band at the concentration of 40 I.U/100 ml while the dendriplexes showed an additional pDNA band at the concentration of 30 I.U/100 ml. Therfore, in comparison to naked dendriplexes, lipodendriplexes showed more resistance against natural polyanions (Fig. 5B).

4.6. Cellular uptake studies

To visualize the transfection efficiency of the optimized dendriplexes and lipodendriplexes, GFP reporter gene expression assay was used. Internalization of complexes was monitored by GFP positive cells to estimate the transfection efficiency showing an overlay of DAPI treated cells coupled to the green fluorescence signal arising from the GFP expression. Cells transfected with lipodendriplexes exhibited a higher green fluorescence signal compared to dendriplexes alone. The higher endosomal release could have contributed towards an increased plasmid GFP transfection through possible cellular events like interactions of nano-complexes with cell membrane, cellular uptake and endosomal release, which results in an efficient entry of pCMV-GFP to the cytoplasm and finally to the nucleus [42] as seen in Fig. 6.

4.7. Chorioallantoic membrane (CAM) analysis

According to the strategy of 3Rs principle (i.e. replacement, refinement, and reduction), different alternative methods should be used to avoid the unethical use of animals. Therefore, at the initial level of research, an alternative method should be first evaluated, which can reduce the exposure of testing drug products on laboratory animals [43]. In the present study, the chorioallantoic membrane (CAM) model was used to evaluate the GFP expression and safety profile of the dendriplexes and lipodendriplexes. The results showed that the lipodendriplexes showed enhanced GFP expression as compared to its parent dendriplexes. The GFP expression was observed in the epithelial cells (Fig. 7). Similar results were obtained by Baghdan et al. [44]. In addition, 48 h post-transfection, the optimized complexes did not produce any toxicity in the developing embryo and showed no injury to the CAM microvasculature. The optimized lipodendriplexes showed efficient transfection along with a good safety profile in the *in ovo* environment.

4.8. Metastatic progression assay

Cancer metastasis is the primary cause of morbidity and mortality and responsible for about 90% of cancer deaths. The disseminated tumour cells play a major role in tumour metastasis, which is not a static process and can invade the nearby organs [45–47]. It has been reported that the plasmid DNA can trigger pro-inflammatory cytokine response (TNF-α, IL-12 and IFN-γ) to produce an anti-tumour effect. The naked plasmid cannot induce cytokine response and requires a vector system to trigger such response [48]. In wound healing assay, cells transfected with lipodendriplexes exhibited less scratch closure as compared to dendriplexes alone (Fig. 8). The percentage of the scratch closure of cells was 100, 94 and 88% for blank, dendriplexes and lipodendriplexes, respectively. From these results, it is clear that the enhanced transfection of pCMV-luc by lipodendriplexes was responsible for the increased cytokine generation and inhibition of metastatic progression. The progression in case of lipodendriplexes without pCMV-luc was similar to the untreated cells (data not shown).

5. Conclusion

In this study, lipodendriplexes were designed by incorporating PAMAM based dendriplexes in a broad range of liposomal formulations. The main objective was to formulate an optimized system for enhanced gene delivery with reduced cytotoxicity. It was observed that the DPPC:CH-PAMAM lipodendriplexes showed a significant improvement in pDNA transfection and cell viability as compared to parent dendriplexes. The optimized lipodendriplexes exhibited higher luciferase gene silencing and cellular uptake with an improved pDNA stability in the presence of competing polyanions as well. They also represented a

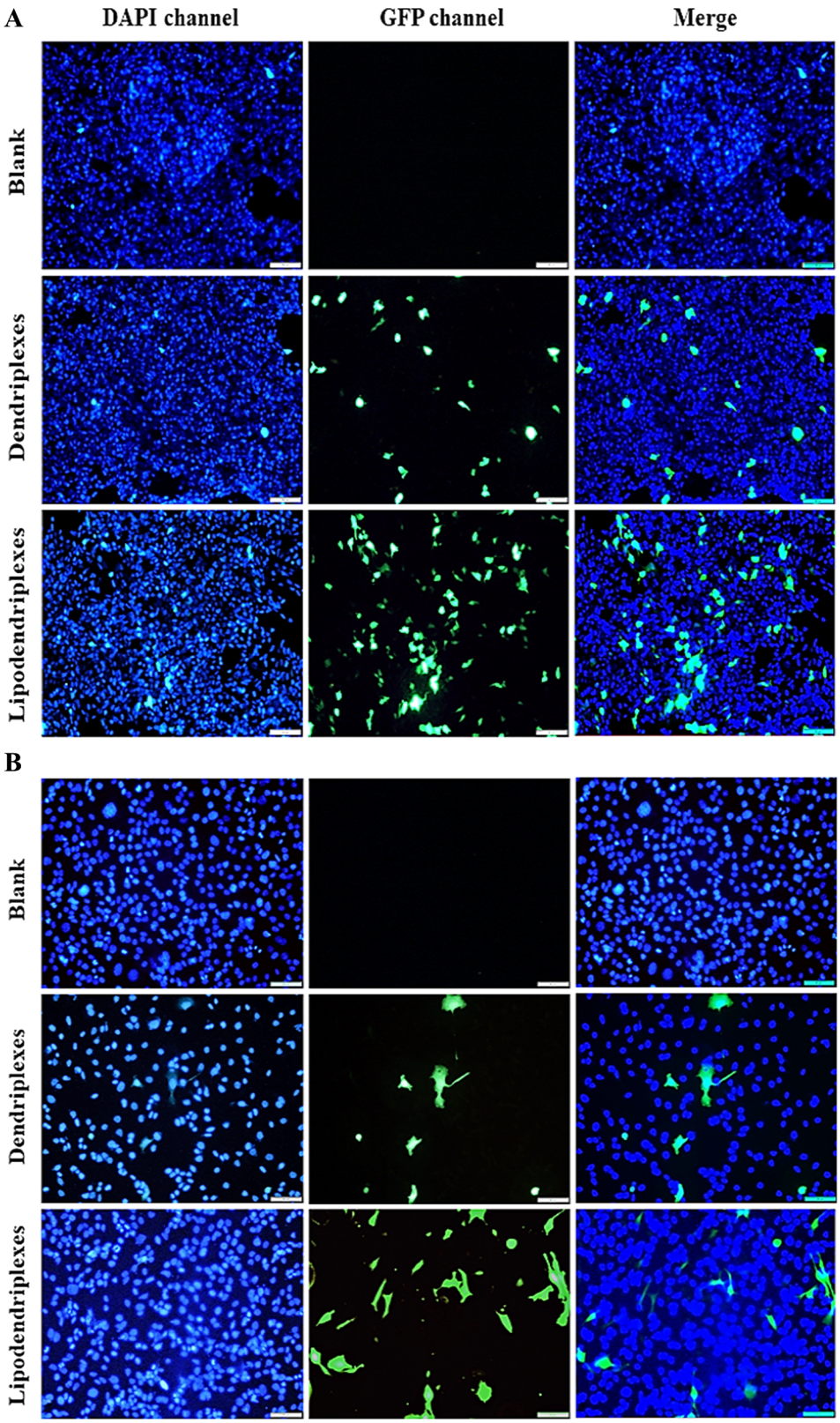

Fig. 6. Fluorescence micrographs with DAPI, GFP and Merged (DAPI + GFP) channels. GFP expression in (A) HEK-293 and (B) SKOV-3 cell lines with optimized dendriplexes (N/P ratio 12) and of DPPC:CH-PAMAM lipodendriplexes (liposome to PAMAM dendrimer mass ratio 0.5). Untransfected cells were considered as blank. Scale bar represents 20 μm.

biocompatible safety profile in hemolysis and CAM experiments. From the findings, it can be concluded that such lipid triblock nanocarrier systems could be potentially important for an improved gene transfection system with a better safety profile. Therefore, further *in vivo* studies to explore the full potential of this platform, using ligand specific targeted systems against different types of cancer and genetic disorders, will be our main objective for future investigations.

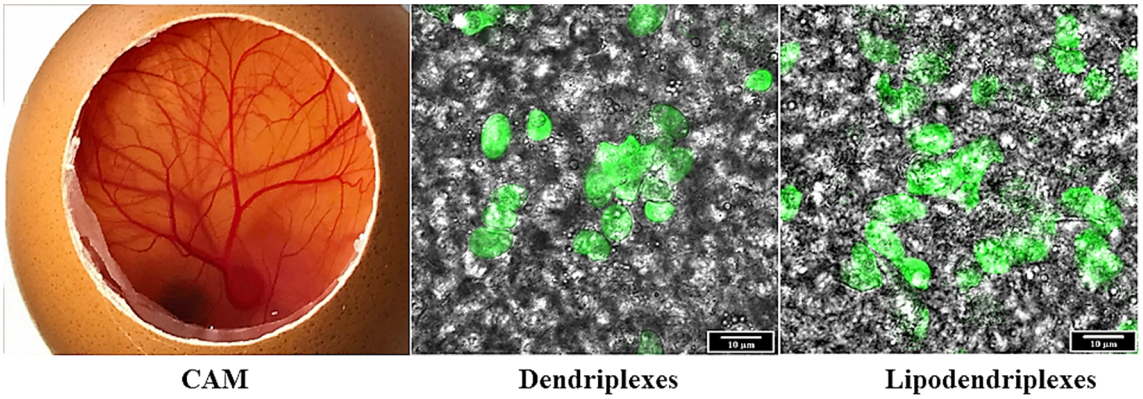

Fig. 7. Apical view of CAM on the egg development day 11 and CLSM micrographs of GFP expression in CAM (epithelial cells) with optimized dendriplexes (N/P ratio 12) and of DPPC:CH-PAMAM lipodendriplexes (liposome to PAMAM dendrimer mass ratio 0.5). Scale bar represents 10 μm.

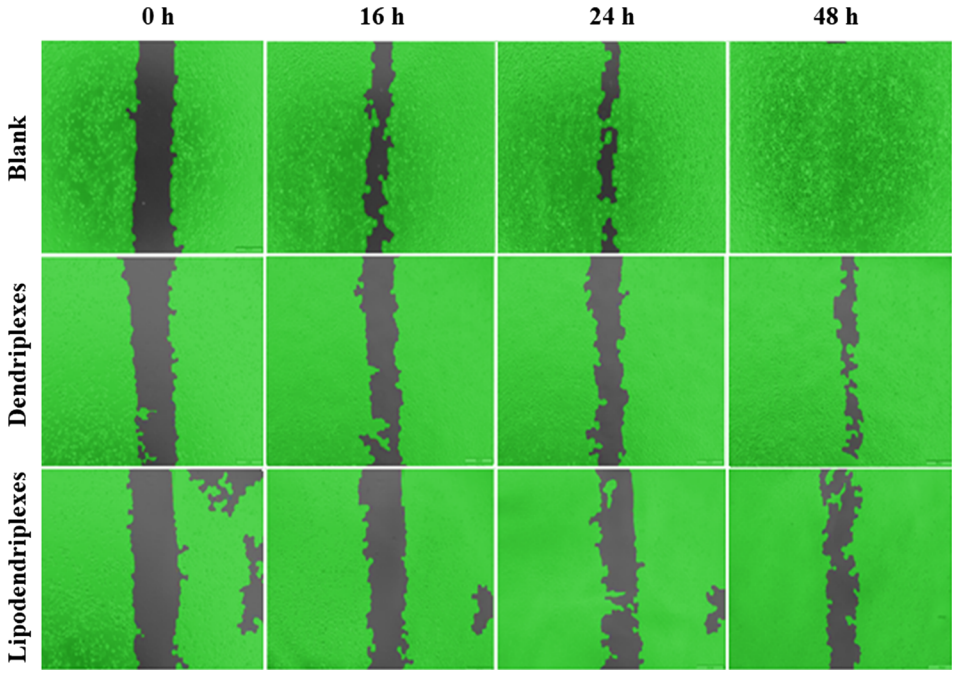

Fig. 8. Metastatic progression assay in SKOV-3 cell line of optimized dendriplexes (N/P ratio 12) and of DPPC:CH-PAMAM lipodendriplexes (liposome to PAMAM dendrimer mass ratio 0.5). Untreated cells were considered as blank. Scale bar represents 100 μm).

Acknowledgment

The authors would like to thank overseas scholarship committee of University of the Punjab and German Academic Exchange Service (DAAD) for providing the scholarship and also Mrs. Eva Maria Mohr for her technical assistance in the cell culture experiments.

References

[1] S.-D. Li, L.-Y. Huang, Nonviral gene therapy: promises and challenges, Gene Ther. 7 (1) (2000) 31–34.
[2] O.M. Merkel, M.A. Mintzer, J. Sitterberg, U. Bakowsky, E.E. Simanek, T. Kissel, Triazine dendrimer as nonviral gene delivery systems: effects of molecular structure on biological activity, Bioconjugate Chem. 20 (9) (2009) 1799–1806.
[3] H. Lv, S. Zhang, B. Wang, S. Cui, J. Yan, Toxicity of cationic lipids and cationic polymers in gene delivery, J. Control. Release 114 (1) (2006) 100–109.
[4] C. Dufes, I.F. Uchegbu, A.G. Schätzlein, Dendrimer in gene delivery, Adv. Drug Deliv. Rev. 57 (15) (2005) 2177–2202.
[5] M.X. Tang, C.T. Redemann, F.C. Szoka, In vitro gene delivery by degraded polyamidoamine dendrimer, Bioconjugate Chem. 7 (6) (1996) 703–714.
[6] H.Y. Nam, H.J. Hahn, K. Nam, W.H. Choi, Y. Jeong, D.E. Kim, J.S. Park, Evaluation of generations 2, 3 and 4 arginine modified PAMAM dendrimer for gene delivery, Int. J. Pharm. 363 (1–2) (2008) 199–205.
[7] M. Labieniec-Watala, K. Karolczak, K. Siewiera, C. Watala, The Janus face of PAMAM dendrimer used to potentially cure nonenzymatic modifications of biomacromolecules in metabolic disorders—A critical review of the pros and cons, Molecules 18 (11) (2013) 13769–13811.
[8] N. Silva Júnior, F. Menacho, M. Chorilli, Dendrimer as potential platform in nanotechnology-based drug delivery systems, IOSR J. Pharm. 2 (5) (2012) 23–30.
[9] T.I. Kim, H.J. Seo, J.S. Choi, H.S. Jang, J.U. Baek, K. Kim, J.S. Park, PAMAM-PEG-PAMAM: novel triblock copolymer as a biocompatible and efficient gene delivery carrier, Biomacromolecules 5 (6) (2004) 2487–2492.
[10] Y.J. Choi, S.J. Kang, Y.J. Kim, Y.B. Lim, H.W. Chung, Comparative studies on the genotoxicity and cytotoxicity of polymeric gene carriers polyethylenimine (PEI) and polyamidoamine (PAMAM) dendrimer in Jurkat T-cells, Drug Chem. Toxicol. 33 (4) (2010) 357–366.
[11] D.W. Pack, A.S. Hoffman, S. Pun, P.S. Stayton, Design and development of polymers for gene delivery, Nat. Rev. Drug Discovery 4 (7) (2005) 581–593.
[12] C.M. Paleos, D. Tsiourvas, Z. Sideratou, A. Pantos, Formation of artificial multicompartment vesosome and dendrosome as prospected drug and gene delivery carriers, J. Control. Release 170 (1) (2013) 141–152.
[13] L.-P. Wu, M. Ficker, J.B. Christensen, P.N. Trohopoulos, S.M. Moghimi, Dendrimer in medicine: therapeutic concepts and pharmaceutical challenges, Bioconjugate Chem. 26 (7) (2015) 1198–1211.
[14] T. Dutta, M. Burgess, N.A. McMillan, H.S. Parekh, Dendrosome-based delivery of siRNA against E6 and E7 oncogenes in cervical cancer, Nanomed.: Nanotechnol. Biol. Med. 6 (3) (2010) 463–470.
[15] S. Kulkarni, G. Betageri, M. Singh, Factors affecting microencapsulation of drugs in liposomes, J. Microencapsul. 12 (3) (1995) 229–246.
[16] M. Gulati, M. Grover, S. Singh, M. Singh, Lipophilic drug derivatives in liposomes, Int. J. Pharm. 165 (2) (1998) 129–168.

[17] T. Nii, F. Ishii, Encapsulation efficiency of water-soluble and insoluble drugs in liposomes prepared by the microencapsulation vesicle method, Int. J. Pharm. 298 (1) (2005) 198–205.
[18] T. Niidome, L. Huang, Gene therapy progress and prospects: nonviral vectors, Gene Ther. 9 (24) (2002) 1647–1652.
[19] A. Ewe, A. Aigner, Nebulization of liposome–polyethylenimine complexes (lipopolyplexes) for DNA or siRNA delivery: physicochemical properties and biological activity, Eur. J. Lipid Sci. Technol. 116 (9) (2014) 1195–1204.
[20] S. Movassaghian, H.R. Moghimi, F.H. Shirazi, A. Koshkaryev, M.S. Trivedi, V.P. Torchilin, Efficient down-regulation of PKC-α gene expression in A549 lung cancer cells mediated by antisense oligodeoxynucleotides in dendrosomes, Int. J. Pharm. 441 (1) (2013) 82–91.
[21] A. Kwok, G.A. Eggimann, J.-L. Reymond, T. Darbre, F. Hollfelder, Peptide dendrimer/lipid hybrid systems are efficient DNA transfection reagents: structure–-activity relationships highlight the role of charge distribution across dendrimer generations, ACS Nano 7 (5) (2013) 4668–4682.
[22] Y. Liu, Y. Ng, M.R. Toh, G.N. Chiu, Lipid-dendrimer hybrid nanosystem as a novel delivery system for paclitaxel to treat ovarian cancer, J. Control. Release 220 (Pt A) (2015) 438–446.
[23] S. Movassaghian, H.R. Moghimi, F.H. Shirazi, V.P. Torchilin, Dendrosome-dendriplex inside liposomes: as a gene delivery system, J. Drug Target. 19 (10) (2011) 925–932.
[24] T. Dutta, M. Garg, N.K. Jain, Poly (propyleneimine) dendrimer and dendrosome mediated genetic immunization against hepatitis B, Vaccine 26 (27) (2008) 3389–3394.
[25] M. Tang, F. Szoka, The influence of polymer structure on the interactions of cationic polymers with DNA and morphology of the resulting complexes, Gene Ther. 4 (8) (1997) 823–832.
[26] S.R. Pinnapireddy, L. Duse, B. Strehlow, J. Schäfer, U. Bakowsky, Composite liposome-PEI/nucleic acid lipopolyplexes for safe and efficient gene delivery and gene knockdown, Colloids Surf. B: Biointerfaces 158 (2017) (2017) 93–101.
[27] K.H. Engelhardt, S.R. Pinnapireddy, E. Baghdan, J. Jedelská, U. Bakowsky, Transfection studies with colloidal systems containing highly purified bipolar tetraether lipids from sulfolobus acidocaldarius, Archaea (2017) 1–12.
[28] F. Lemarié, D.R. Croft, R.J. Tate, K.M. Ryan, C. Dufès, Tumor regression following intravenous administration of a tumor-targeted p73 gene delivery system, Biomaterials 33 (9) (2012) 2701–2709.
[29] B.C. Evans, C.E. Nelson, S.Y. Shann, K.R. Beavers, A.J. Kim, H. Li, H.M. Nelson, T.D. Giorgio, C.L. Duvall, Ex vivo red blood cell hemolysis assay for the evaluation of pH-responsive endosomolytic agents for cytosolic delivery of biomacromolecular drugs, J. Visual. Experim. JoVE (73) (2013) 1–5.
[30] L. Duse, S.R. Pinnapireddy, B. Strehlow, J. Jedelská, U. Bakowsky, Low level LED photodynamic therapy using curcumin loaded tetraether liposomes, Eur. J. Pharm. Biopharm. 126 (2018) (2017) 233–241.
[31] S. Pinnapireddy, L. Duse, D. Akbari, U. Bakowsky, Photo-enhanced delivery of genetic material using curcumin loaded composite nanocarriers, Clin. Oncol. 2 (2017) 1–5.
[32] J. Nguyen, X. Xie, M. Neu, R. Dumitrascu, R. Reul, J. Sitterberg, U. Bakowsky, R. Schermuly, L. Fink, T. Schmehl, T. Gessler, Effects of cell penetrating peptides and pegylation on transfection efficiency of polyethylenimine in mouse lungs, J. Gene Med. 10 (11) (2008) 1236–1246.
[33] P.K. Maiti, T. Çağın, S.-T. Lin, W.A. Goddard, Effect of solvent and pH on the structure of PAMAM dendrimer, Macromolecules 38 (3) (2005) 979–991.
[34] H.K. Alajangi, P. Natarajan, M. Vij, M. Ganguli, D. Santhiya, Role of unmodified low generation–PAMAM dendrimer in efficient non toxic gene transfection, Chem. Select 1 (16) (2016) 5206–5217.
[35] A. Kumar, V.K. Yellepeddi, G.E. Davies, K.B. Strychar, S. Palakurthi, Enhanced gene transfection efficiency by polyamidoamine (PAMAM) dendrimer modified with ornithine residues, Int. J. Pharm. 392 (1) (2010) 294–303.
[36] T. Dutta, H.B. Aghase, P. Vijayarajkumar, M. Joshi, N.K. Jain, Dendrosome-based gene delivery, J. Exp. Nanosci. 1 (2) (2006) 235–248.
[37] Y. Zhang, H. Li, J. Sun, J. Gao, W. Liu, B. Li, Y. Guo, J. Chen, DC-Chol/DOPE cationic liposomes: a comparative study of the influence factors on plasmid pDNA and siRNA gene delivery, Int. J. Pharm. 390 (2) (2010) 198–207.
[38] P. Laskar, S. Somani, N. Altwaijry, M. Mullin, D. Bowering, M. Warzecha, K. Patricia, J.T. Rothwelle, L. Hing, C. Dufes, Redox-sensitive, cholesterol-bearing PEGylated poly (propyleneimine)-based dendrimersomes for drug and gene delivery to cancer cells, Nanoscale (2018), https://doi.org/10.1039/C8NR08141G.
[39] J. Schäfer, S. Höbel, U. Bakowsky, A. Aigner, Liposome–polyethylenimine complexes for enhanced DNA and siRNA delivery, Biomaterials 31 (26) (2010) 6892–6900.
[40] B. Birdhariya, P. Kesharwani, N.K. Jain, Effect of surface capping on targeting potential of folate decorated poly (propylene imine) dendrimer, Drug Dev. Ind. Pharm. 41 (8) (2015) 1393–1399.
[41] H. Engelberg, Plasma heparin levels, Circulation 23 (4) (1961) 573–577.
[42] N. Golkar, S.M. Samani, A.M. Tamaddon, CH-conjugated supramolecular assemblies of low generations polyamidoamine dendrimer for enhanced EGFP plasmid DNA transfection, J. Nanopart. Res. 18 (5) (2016) 1–20.
[43] S.K. Doke, S.C. Dhawale, Alternatives to animal testing: a review, Saudi Pharm. J. 23 (3) (2015) 223–229.
[44] E. Baghdan, S.R. Pinnapireddy, B. Strehlow, K.H. Engelhardt, J. Schäfer, U. Bakowsky, Lipid coated chitosan-DNA nanoparticles for enhanced gene delivery, Int. J. Pharm. 535 (1) (2018) 473–479.
[45] X. Guan, Cancer metastases: challenges and opportunities, Acta Pharmaceutica Sinica B 5 (5) (2015) 402–418.
[46] P.C. Hermann, S.L. Huber, T. Herrler, A. Aicher, J.W. Ellwart, M. Guba, C.J. Bruns, C. Heeschen, Distinct populations of cancer stem cells determine tumor growth and metastatic activity in human pancreatic cancer, Cell Stem Cell 1 (3) (2007) 313–323.
[47] H. Yamaguchi, J. Wyckoff, J. Condeelis, Cell migration in tumors, Curr. Opin. Cell Biol. 17 (5) (2005) 559–564.
[48] M. Whitmore, S. Li, L. Huang, LPD lipopolyplex initiates a potent cytokine response and inhibits tumor growth, Gene Ther. 6 (11) (1999) 1867–1875.